Pflugers Arch - Eur J Physiol (2014) 466:2205–2214
DOI 10.1007/s00424-014-1492-4

ION CHANNELS, RECEPTORS AND TRANSPORTERS

T-type Ca^{2+} channels facilitate NO-formation, vasodilatation and NO-mediated modulation of blood pressure

Per Svenningsen · Kenneth Andersen · Anne D. Thuesen · Hee-Sup Shin · Paul M. Vanhoutte · Ole Skøtt · Boye L. Jensen · Caryl Hill · Pernille B. L. Hansen

Received: 24 January 2014 / Revised: 25 February 2014 / Accepted: 26 February 2014 / Published online: 14 March 2014

Abstract Voltage-gated calcium channels are involved in the vascular excitation-contraction mechanism and regulation of arterial blood pressure. It was hypothesized that T-type channels promote formation of nitric oxide from the endothelium. The present experiments determine the involvement of T-type channels in depolarization-dependent dilatation of mesenteric arteries and blood pressure regulation in Cav3.1 knock-out mice. Nitric oxide-dependent vasodilatation following depolarization-mediated vasoconstriction was reduced significantly in mesenteric arteries from $Cav3.1^{-/-}$ compared to wild type mice. Four days of systemic infusion of a nitric oxide (NO)-synthase-inhibitor to conscious wild type elicited a significant increase in mean arterial blood pressure that was absent in $Cav3.1^{-/-}$ mice. Immunoprecipitation and immunofluorescence labeling showed co-localization of Cav3.1 and endothelial nitric oxide synthase (eNOS) in arteries from wild type mice. Nitric oxide release measured as DAF fluorescence and cGMP levels were significantly lower in depolarized $Cav3.1^{-/-}$ compared to wild type arteries. In summary, the absence of T-type Cav3.1 channels attenuates NO-dependent dilatation in mesenteric arteries in vitro, as well as the hypertension after L-NAME infusion in vivo. Furthermore, Cav3.1 channels cluster with eNOS and promote formation of nitric oxide by the endothelium. The present findings suggest that this mechanism is important for the systemic impact of NO on peripheral resistance.

Keywords Resistance · Hypertension · Depolarization · L-type

Introduction

The regulation of arterial blood pressure is multifactorial and involves several organs. Arterioles contribute to the reflex control of blood pressure by regulated changes of their inner diameter producing changes in peripheral vascular resistance. Several types of calcium channels including T-type channels are involved in the excitation-contraction coupling in blood vessels of both rodents and humans [10, 21, 11, 3, 1]. In contrast, recent studies of perfused mouse renal efferent arterioles showed unexpectedly that T-type voltage-gated channels also contribute to endothelium-dependent vasodilatation following depolarization-induced calcium influx [24]. However, it is not known whether this latter finding in the renal microcirculation represent a more general phenomenon to restrict excessive vasoconstriction and stabilize blood pressure. If so, then knowledge of the mechanism underlying this T-type channel-mediated vasodilatation could have potential therapeutic application. The potential mechanism(s) involved in the secondary dilatation to depolarization is not clear, although endothelium-dependent hyperpolarization does not

Electronic supplementary material The online version of this article (doi:10.1007/s00424-014-1492-4) contains supplementary material, which is available to authorized users.

P. Svenningsen · K. Andersen · A. D. Thuesen · O. Skøtt · B. L. Jensen · P. B. L. Hansen (✉)
Department of Cardiovascular and Renal Research, University of Southern Denmark, Winsløwparken 21, 3, Odense DK-5000, Denmark
e-mail: pbhansen@health.sdu.dk

H.-S. Shin
Center for Cognition and Sociality, Institute for Basic Science, Seoul, South Korea

P. M. Vanhoutte
Department of Pharmacology and Pharmacy and State Key Laboratory for Pharmaceutical Biotechnology, Li Ka Shing Faculty of Medicine, University of Hong Kong, Hong Kong, China

C. Hill
John Curtin School of Medical Research, Australian National University, Canberra, ACT, Australia

appear contribute to the T-type channel-mediated dilatation in response to a high extracellular potassium concentration [24], making nitric oxide (NO) the likely mediator.

Two molecular subtypes of T-type channels (Cav3.1 and Cav3.2) have been identified in the vasculature. The present study focuses on the potential role of the Cav3.1 subtype T-type mediated endothelium-dependent dilatation. This channel is encoded by the CACNA1G gene which is subject to extensive splice variation capable of altering membrane expression and biophysical properties of the channels [26, 17, 31]. Mice deficient in Cav3.1 channels exhibit sleep disturbances [18], defective vascular smooth muscle cell proliferation [28] and bradycardia. Targeted deletion of Cav3.1 gene in mice causes slowing of heart rate but has no effect on mean arterial blood pressure [19], indicating a higher peripheral vascular resistance buffered by a reflex lowering of heart rate. Taken in conjunction, these data suggest that opening of Cav3.1 T-type channels may lead to vasodilatation through a hitherto unknown direct stimulation of nitric oxide formation.

The present study was therefore designed to determine whether or not Cav3.1 channels can contribute to endothelium-dependent dilatations of systemic resistance vessels and, if so, to investigate the mechanism(s) involved in this response. In particular, the hypothesis was tested that these T-type channels can be involved in dilatation of resistance vessels through activation of endothelial nitric oxide synthase (eNOS). To address these questions directly, isolated mesenteric arteries were stimulated with an elevated potassium ion concentration to activate voltage-gated calcium channels. The resultant vascular responses were compared in preparations of mice with or without targeted disruption of Cav3.1 channels. The role of Cav3.1 channels in nitric oxide-mediated modulation of blood pressure was also tested in these mice by continuously monitoring arterial blood pressure and heart rate in unrestrained conscious animals.

Materials and methods

The animal experimental protocol was approved by the Danish Animal Experiments Inspectorate under the Danish Ministry of Justice and animal care followed the guidelines of the National Institutes of Health. Studies were conducted in male and female Cav3.1$^{-/-}$ mice [18] and C57BL/6J wild type mice were used as controls (Taconic Farm Inc., Ry, Denmark) as Cav3.1$^{-/-}$ mice were backcrossed to a C57BL/6 background for more than ten generations. eNOS$^{-/-}$ mice were used to test the involvement of NO (C57BL/6 background, backcrossed for more than ten generations, Jackson Laboratory). An equal number of male and female mice were included in all experimental groups. The animals were from 8 to 10 weeks of age and were kept on a 12:12-h light: dark cycle with free access to normal chow and tap water.

Isolation and microperfusion of mesenteric resistance arteries

Mesenteric arteries from mice killed by cervical dislocation were dissected in physiological saline solution (PSS, 4 °C) and transferred in a pipette to a thermostated chamber (Warner Instruments, Hamden, CT, USA). The specimen was mounted on a set of glass pipettes using 11-0 sutures and pressurized to 60 mmHg at the inlet and 55 mmHg at the outlet pipette, resulting in perfusion with PSS with a flow rate of 1–2 μL/min. The chamber was mounted on an inverted microscope (Zeiss Axiovert 10, Oberkochen, Germany). The experiments were recorded using a Till Photonics (Munich, Germany) video camera and software. The luminal diameter was determined at the most reactive part of the blood vessel. All experimental protocols started with a period of equilibration after the perfusion was established (37 °C, saturated 5 % CO_2 in air), and viability was tested by administration of a high potassium physiological saline solution (HPS; 70 mmol/L KCl) added to the organ chamber. Phentolamine (10^{-5} mol/L) was added to all solutions to exclude nerve-mediated α-adrenergic effects of depolarization. Secondary dilatation represents the difference in diameter from maximal constriction to the diameter after the subsequent dilatation occurring in the presence of high K^+ calculated as

$$\text{Secondary dilatation } (\%) = \frac{D_{\text{min+30sec}} - D_{\text{min}}}{D_{\text{rest}} - D_{\text{min}}} \cdot 100$$

where D_{min} is the minimum diameter (maximum constriction) after depolarization, $D_{\text{min+30}}$ is the diameter 30 s after maximum constriction and D_{rest} is the resting diameter.

The following protocols were conducted in WT (C57BL/6J) and Cav3.1$^{-/-}$ mice. High potassium solution (HPS) was added for 3 min and secondary dilatation determined after 60 and 180 s. To test for the potential involvement of NO release, the NOS inhibitor L-NAME (10^{-4} mol/L; Sigma-Aldrich, Schnelldorf, Germany) was applied to the chamber for 20 min followed by HPS; the effect of HPS on secondary dilatation was also tested in arteries of eNOS$^{-/-}$ mice. Furthermore, the effect of an NO donor, sodium nitroprusside (SNP, 10^{-7} mol/L; Sigma-Aldrich), was examined by administration of SNP for 120 s 1 min after high potassium administration. In the next series of experiments, the dilator response to 120 s of exposure to isoprenaline (10^{-7} mol/L, Sigma-Aldrich) was investigated in HPS preconstricted blood vessels. This experiment was repeated in the presence of the beta-adrenoceptor blocker propranolol (10^{-6} mol/L; Sigma-Aldrich). To further investigate whether or not gap junctions were involved in the response, arteries were incubated for 45 min with 18α-glycyrrhetinic acid (2×10^{-5} mol/L; Sigma-Aldrich) prior to HPS application. Finally, to determine acetylcholine-induced responses preparations from the

different mouse genotypes were constricted with HPS for 1 min and acetylcholine (10^{-6} mol/L; Sigma-Aldrich) was applied for 120 s in the absence or presence of L-NAME (10^{-4} mol/L). To distinguish agonist-mediated dilatation from secondary dilatation (depolarization induced dilatation) the dilatation was calculated as

$$\text{Dilatation } (\%) = \frac{D_{\min+195\text{sec}} - D_{\min}}{D_{\text{rest}} - D_{\min}} \cdot 100$$

where $D_{\min}$ is the minimum diameter (maximum constriction) after depolarization, $D_{\min+30}$ is the diameter 30 s after maximum constriction and D_{rest} is the resting diameter.

Saline solutions PSS contained in mmol/L: NaCl 115, $NaHCO_3$ 25, $MgSO_4$ 1.2, $K2HPO_4$ 2.5, $CaCl_2$ 1.3, glucose 5.5 and HEPES 10. HPS contained in mM: NaCl 45, KCl 70, $NaHCO_3$ 25, $MgSO_4$ 1.2, $K2HPO_4$ 2.5, $CaCl_2$ 1.3, glucose 5.5 and HEPES 10. The solutions were equilibrated with 5 % CO_2 in air resulting in a pH=7.4 with 0.1 and 1 % bovine serum albumin superfusate and perfusate, respectively.

In vivo experiments: arterial blood pressure and heart rate measurements in conscious mice

Mice were anaesthetized (Ketamin 100 mg/kg/Xylazine 10 mg/kg) and chronic indwelling catheters were placed in the femoral artery and vein for measurements of arterial blood pressure and drug infusions, respectively [2, 9]. Arterial and venous catheters consisted of a Micro-Renathane tip connected to a polyethylene tubing. The catheters were exteriorized through a subcutaneous tunnel from the groin to the neck, and the catheters were attached to a swivel enabling the mice to move freely. To maintain catheter patency, a heparin solution (100 IU/mL in isotonic glucose) was infused (10 μL/h) at the arterial side. The mice recovered for 5 days before beginning the continuous measurements of mean arterial blood pressure and heart rate; at that time, they had fully recovered and no change in blood pressure and heart rate were observed during the following days. The actual experiments were initiated by connecting the arterial line to a pressure transducer (Föhr Medical Instruments, Hessen, Germany), and data were collected at 200 Hz using Lab View software (National Instruments, Austin, TX, USA).

Protocol Mean arterial blood pressure (MAP) and heart rate were measured continuously for 2 days followed by a bolus injection of isotonic glucose (50 μL) through the venous catheter to place L-NAME in the dead space of the catheter. L-NAME (10 mg/kg/day) was infused at a rate of 10 μL/h for 3 days. L-NAME was administered to WT and $Cav3.1^{-/-}$ mice. Two hundred microliters of blood was collected from the artery line before termination of the experiment. The data are presented as increase in mean arterial blood pressure after L-NAME infusion for 24, 48 and 72 h calculated as the difference in MAP before and after infusion. The data include all MAP measurements during the given time period.

Plasma nitrite

Nitrite was determined using a Nitrate/Nitrite Colorimetric Assay Kit (780001, Cayman Chemical, Michigan, USA). Blood samples were diluted 1:2 and run in duplicate.

Immunoprecipitation

Mouse aortic arteries were isolated and snap frozen in liquid nitrogen for storage. Aortae were used instead of mesenteric arteries to get enough tissue for the following protocol. Vessels were fixed in 4 % paraformaldehyde, washed and chopped into small pieces and transferred to 1×IP buffer with protease inhibitor cocktail (Roche, Palo Alto, CA). The lysates were precleared by centrifugation at 12,000*g* for 5 min at 4 °C and transferred to a spin column (#IP50; Sigma-Aldrich). The lysate was mixed with 5 μg of primary antibody [α_{1G} (Alomone Labs, Jerusalem, Israel, #ACC-021), eNOS (R&D Systems, #AF950) and IgG (DakoCytomation, Glostrup, Denmark)], followed by incubation at 4 °C overnight. Protein G Sepharose 4B Fast Flow, recombinant protein G beads (Sigma-Aldrich, #IP50) were administered for 2–3 h at 4 °C. The samples were first washed twice with 1×IP buffer with 0.5 M NaCl, 0.1 % SDS, then four times with 1×IP buffer and then one time with 0.1×IP buffer. The samples were precipitated with 0.1×IP buffer with lithium dodecyl sulfate (LDS) and loading buffer (Invitrogen, Naerum, Denmark) before SDS-PAGE electrophoresis (4–15 %, Tris-HCl gels, Bio-Rad, Copenhagen, Denmark), followed by transfer to an Immobilin-P PVDF-membrane (0.45 μm pore-size, Millipore, Copenhagen, Denmark) using the XCell SureLock Mini-Cell system (Invitrogen). Membranes were blocked for 1 h with 5 % nonfat milk in TBST (20 mM Tris-base (Sigma Aldrich), 137 mM NaCl, 0.05 % Tween 20 (Sigma Aldrich), pH 7.6) and incubated at 4 °C overnight with α_{1G} polyclonal (1:500, Millipore, #AB5491-200UL) or eNOS (1:500). Incubation with goat anti-rabbit horseradish peroxidase (HRP) or rabbit anti-goat horse radish peroxidase (HRP) secondary antibodies was performed at room temperature (1:5,000, Dako, Glostrup, Denmark). Blots were exposed to developing agent.

Western blotting

Aortae were homogenized in 0.3 M sucrose, 25 mM imidazole, 1 mM EDTA disodium salt, 0.4 M Pefabloc, 2.1 mM Leupeptin, 1 mM Na-orthovanadate, 0.2 M NaF and 0.082 μg/μL okadaic acid. Protein concentrations were

determined using the Lowry Protein Assay (Bio-Rad, Hercules, USA). Protein (30 μg) was separated by SDS-PAGE and blotting performed as described above. Membranes were incubated overnight at 4 °C with primary antibody; Phospho-eNOS (serine 1177) (9571, Cell Signaling Technology, Millipore, Copenhagen, Denmark) diluted 1:1,000 in 5 % milk in TBST followed by incubation with HRP-conjugated secondary antibody directed against goat IgG (P0449, Dako, Glostrup, Denmark; 1:2,000). Labeling was visualized by the ECL plus Western Blotting Detection System (Amersham Biosciences/GE Healthcare, Munich, Germany). Optical densities of the bands were determined with Quantity One 4.03 software (Bio-Rad). To confirm equal protein loading, membranes were stripped (TBST, pH 2) 2× 10 min, blocked and loaded with an antibody against β-actin (1:2,000, Abcam, Cambridge, UK).

Immunofluorescence labeling of whole-mount mesenteric arteries and aortae

The localization of Cav3.1 expression was tested in mouse aortas and mesenteric arteries using two different protocols. Aortae and mesenteric arteries were dissected from wild type mice, and the former were split open. In the first protocol, the arteries were immediately fixed in 4 % formaldehyde/PBS for 10 min at room temperature, and washed once in phosphate buffer solution (PBS). The arteries were subsequently blocked and permeabilized with PBS (Invitrogen), 0.1 % Triton X-100 (Sigma Aldrich), 1 % BSA (Sigma Aldrich) for 1 hour at room temperature. The arteries were then incubated overnight with α_{1G} (1:100, Alomone Labs, or Millipore) and eNOS (1:50) antibodies at 4 °C. They then washed, incubated with secondary antibodies (Alexa-594 donkey anti-rabbit and Alexa-488 donkey anti-goat, Invitrogen) for 1 hour at room temperature, washed again and counterstained with DAPI (Sigma Aldrich). The second protocol was based on the previously described method [16]. Briefly, arteries were immersed in 30 % sucrose for 10 min and subsequently incubated in rabbit anti-Cav3.1 (1:500, kindly provided by Dr Leanne Cribbs, Loyola University, Chicago, IL, USA) and goat anti-eNOS (1:50) in 2 % bovine serum albumin, 0.2 % Triton X in PBS (24 to 72 h, 4 °C). The primary antibodies were visualized by incubating the arteries in Alexa-546 donkey anti-rabbit and Alexa-488 donkey anti-goat (Invitrogen) for 24 h at 4 °C). The arteries the counterstained with DAPI and mounted on glass slides. Images were acquired with confocal laser-scanning fluorescence microscopy (Olympus FV1000, Hamburg, Germany) using a ×20 (numerical aperture, 0.95) Olympus water immersion objective. Full-frame imaging was performed using sequential excitation from a laser at 405, 488 and 559 nm with fluorescence emission monitored through appropriate acousto-optic tunable filters settings. The images were subsequently processed using ImageJ version 1.40 g. Specificity of the immunolabeling was tested by omitting the primary antibody.

DAF measurements

Mesenteric arteries from mice were isolated as described above. The arteries were cut open and transferred to a thermostated chamber with physiological saline solution (PSS). The arteries were placed with the endothelial cells facing upwards. All experimental protocols started with a resting period of 30 min for equilibration (37 °C, saturated 5 % CO2 in air), 45 min of incubation with 4 μM diaminofluorescein (DAF)-FM diacetate (Molecular Probes®) in 0.1 % DMSO followed by 15 min wash-out with PSS for de-esterification. Phentolamine (10^{-5} mol/L) was added to all solutions. The chamber was mounted on an inverted microscope (Olympus IX71). The experiments were visualized by excitation at 495 nm and emission at 515 nm using Olympus X20 (0.45 numerical aperture) objective. Full-frame images were collected and analyzed for relative changes in fluorescence intensity ($\Delta F=(F/F0)$) using XCellence rt (Olympus Soft Imaging Solution GmbH). Endothelial cells that were in focus during the whole experiment were analyzed.

Tissue cGMP

Aortae were isolated from WT and Cav3.1$^{-/-}$ mice and the blood vessels incubated for 2 min in either PPS or HPS. The tissue was then transferred to liquid nitrogen and stored at −80 °C. Tissue from 4 mm of vessel was homogenized with a mortar and pestle in liquid nitrogen. The cyclic guanosine monophosphate (cGMP) content was then measured with a cyclic GMP EIA kit (Cayman Chemicals) according to the manufacturer's instructions. In short, the pulverized tissue was transferred to a test tube containing 150 μL of 5 % trichloroacetic acid in water. The trichloroacetic acid of the supernatant was then extracted with ether, and the remaining cGMP was acetylated. The pellet was dried, weighed and the cGMP concentration expressed in proportion to dry weight.

Real-time PCR

RNA was isolated from mouse aortae and mesenteric arteries (WT and Cav3.1$^{-/-}$). Aortae were chopped up or mesenteric arteries crushed in a mortar before adding TRIzol reagent from Invitrogen (Copenhagen, Denmark) and reverse transcribed using Iscript (Bio-Rad). Quantitative three-step real-time PCR was performed on a Mx3000 real-time PCR instrument using 2X IQ SYBR Green Supermix (Bio-Rad) according to the manufacturer's instructions. All measurements were performed in duplicate. Real-time PCR consisted of 40 cycles and each cycle included incubation at 95ºC for 20 s, 60ºC for 20 s and 72ºC for 20 s. Specific primers were used for eNOS,

CD31, Cav1.2, Cav3.1 and Cav3.2, and the results were normalized to the housekeeping gene Tbcc. Mouse primers eNOS (Genbank no: NM008713, sense 5′-GAG AGC GAG CTG GTG TTT G-3′ and antisense 5′-TGA TGG CTG AAC GAA GAT TG-3′ covering 189 bp), CD31 (Genbank no: NM008816XX, sense 5′-AGA GAC GGT CTT GTC GCA GT-3′ and antisense 5′-AAT GCT CTC GAA GCC CAG TA-3′ covering 152 bp), Cav1.2 (Genbank no: NM009781 sense 5′-TGC CTA CGG ACT TCT CTT CC-3′ and antisense 5′-GCT CCT TTC CCT CCT AGA GC-3′ covering 150 bp), Cav3.1(Genbank no: NM 009783 sense 5′-CCC CGG TGG TTT TCT TCT AC-3′ and antisense 5′-CAC AGG CAA TGT CCT CAC AC-3′ covering 159 bp), Cav3.2 (Genbank no: NM 021415 sense 5′-CTC ACA ATG GTG CCA TCA AAC-3′ antisense 5′-TGG GCA TCC ATG ACG TAG TA-3′ covering 112 bp) and Tbcc (Genbank no: NM_178385, sense 5′-GAC TCC TTC CTG AAC CTC TGG-3′ and antisense 5′-GGA GGC CAT TCA AAA CTT CA-3′ covering 189 bp).

Negative controls included water and RNA where no reverse transcriptase was added to the reaction (−RT). Positive control was whole kidney tissue (mouse).

Statistical analysis

Data are presented as means±SEM. Significance of changes was calculated by two-way analysis of variance (ANOVA) with Bonferroni reduction for multiple comparisons and Student's *t*-test for comparison of two groups. *P* values less than 0.05 were considered to indicate statistically significant differences.

Results

Depolarization induced responses in mesenteric arteries from T-type knock-out mice

The contribution of Cav3.1 channels in the dilatation following the depolarization-induced constriction (hereafter referred to as secondary dilatation) was studied in isolated mesenteric arteries of T-type calcium channel deficient mice ($Cav3.1^{-/-}$). The resting basal diameter of mesenteric arteries averaged (n=6) 210±22 and 223±12 μm in WT and $Cav3.1^{-/-}$, respectively. In all experiments, high potassium solution (HPS) elicited a large transient constriction followed by a secondary dilatation. The average HPS-induced constriction did not differ amongst the genotypes (change in diameter, WT 127±16 μm and $Cav3.1^{-/-}$ 127±10 μm; Fig. 1a). The secondary dilatation which occurred in the presence of HPS was significantly lower in $Cav3.1^{-/-}$ compared to WTs preparations after both 1 and 3 min of exposure (Fig. 1b).

Secondary vasodilatation, measured after 1 min of HPS exposure was abolished by L-NAME in mesenteric arteries from WT and $Cav3.1^{-/-}$ and absent in mesenteric arteries from $eNOS^{-/-}$ mice (Fig. 2a). Addition of the NO donor SNP significantly increased the HPS-induced secondary vasodilatation in vessels from $Cav3.1^{-/-}$ mice but not WT mice (increase in secondary dilatation after SNP: $Cav3.1^{-/-}$ 49±14 % and WT 11.8±10 %) in $Cav3.1^{-/-}$ (Fig. 2b). Incubation with the gap junction blocker 18α-glycyrrhetinic acid did not significantly change the secondary dilatation after HPS in wild type mice (Fig. 2c).

The ability of the $Cav3.1^{-/-}$ arteries to dilate was tested using acetylcholine (10^{-6} M) and isoprenaline (10^{-7} M) after HPS-induced contraction and secondary dilatation. Arteries dilated in response to acetylcholine on average to 87±7 μm in WT with a similar dilatation observed in $Cav3.1^{-/-}$ (Fig. 2d). Isoprenaline also significantly increased the luminal diameter and to a comparable extent in both WT and $Cav3.1^{-/-}$ (Online Resource 1). Propranolol inhibited the isoprenaline-elicited response (data not shown).

Effect of NOS inhibition on mean arterial blood pressure and heart rate

Mean arterial blood pressure (MAP) and heart rate were measured over 6 days in WT and $Cav3.1^{-/-}$ (Fig. 3a, b). The resting basal MAP measured for the first two days averaged 100.5±1.7 and 100.5±6.3 mmHg in WT and $Cav3.1^{-/-}$, respectively (n=6) with no significant difference between sexes. A tendency to circadian rhythm was observed in both genotypes. L-NAME infusion caused a significant increase in MAP and decrease in HR in WT mice, whereas $Cav3.1^{-/-}$ mice did not exhibit a significant increase in MAP (Fig. 3c). The plasma nitrite/nitrate concentration was not significantly different between the WT and $Cav3.1^{-/-}$ mice at the end of the experiment (WT 11.9±2.4 μM and $Cav3.1^{-/-}$ 12.7±4.9 μM).

Localization of eNOS and Cav in arteries

eNOS is activated directly by increases in intracellular calcium, and it was therefore tested if the T-type channels co-localize with eNOS. Immunoprecipitation of eNOS pulled down Cav3.1 (n=4) and immunoprecipitation of Cav3.1 pulled down eNOS (n=3) (Fig. 4a). eNOS is also activated by phosphorylation of serine 1177; however, at baseline, no difference in eNOS-pS1177 levels was observed between wild type and $Cav3.1^{-/-}$ mice (Fig. 4b).

Confocal laser-scanning microscopy of mesenteric arteries showed co-localization of eNOS and Cav3.1 also in endothelial cells of mesenteric arteries (Fig. 4c). The staining expression pattern of Cav3.1 was confirmed using three separate primary antibodies. In agreement, confocal laser-scanning microscopy of isolated aortae immunofluorescence-labeled with antibodies against eNOS and Cav3.1 confirmed the co-localization of eNOS and Cav3.1 in endothelial cells and

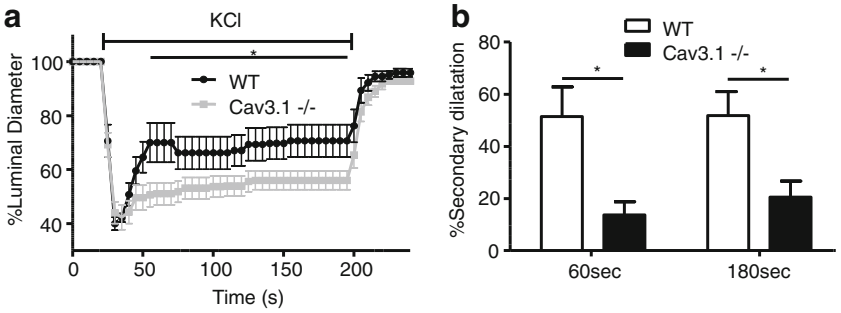

Fig. 1 Depolarization-induced constriction and subsequent dilatation in mouse mesenteric arteries. **a** Changes in luminal diameter after administration of K^+ (70 mM) to isolated mesenteric arteries from Cav3.1$^{-/-}$ mice and C57BL/6 (WT). **b** Subsequent dilatation after K^+ (secondary dilatation) measured after 60 or 180 s of K^+ administration in Cav3.1$^{-/-}$ mice and C57BL/6 (WT). Data are means±SEM, n=6;*P<0.05. The *bare* under the *asterisk* show significant different time point (1**a**)

showed that Cav3.1was also expressed in vascular smooth muscle cells (Fig. 4d and Online Resource 2).

NO and cGMP measurements

NO measurements using fluorescent imaging with DAF-FM showed a significantly higher NO production in mesenteric arteries of WT compared to Cav3.1$^{-/-}$ mice following exposure to HPS (Fig. 5a, c). Both increases were abolished by L-NAME (Fig. 5b, c). HPS increased NO levels by 50 % in mesenteric vessels from wild type mice whereas NO levels increased by 25 % in Cav3.1$^{-/-}$ vessels (Fig. 5c). Furthermore, DAF fluorescence was significantly different from baseline after 20 s (p<0.05) in WT, whereas Cav3.1$^{-/-}$ vessels were only significantly different from baseline at 43 s after depolarization. Although baseline cGMP levels in isolated aortae were not different between Cav3.1$^{-/-}$ and WT mice (data not shown) stimulation with HPS led to significantly higher levels of cGMP in WT compared to Cav3.1$^{-/-}$ mice (Fig. 5d). Together these data confirmed a smaller NO production in Cav3.1$^{-/-}$ than in WT mice.

mRNA expression of Cav isoforms and eNOS

The messenger RNA (mRNA) levels of eNOS were not significant different in either isolated mesenteric arteries or isolated aortae from Cav3.1$^{-/-}$ compared to wild type mice (Online Resource 3a, b). The amount of endothelial cells as

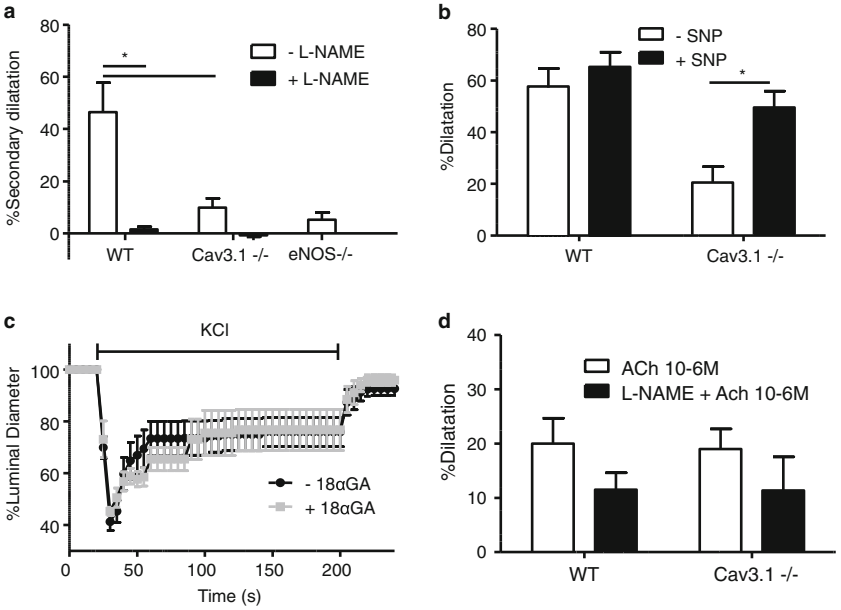

Fig. 2 Involvement of NO in the depolarization induced dilatation in mesenteric arteries. **a** Secondary dilatation measured after administration of K^+ for 60 s in the presence and absence of the NO synthases inhibitor L-NAME in WT and Cav3.1$^{-/-}$ mice and in eNOS$^{-/-}$ mice. **b** Dilatation in response to 2 min administration of sodium nitroprusside (SNP) to K^+ constricted arteries from WT and Cav3.1$^{-/-}$ mice. **c** Changes in luminal diameter of WT blood vessels after administration of K^+ (70 mM) in the presence and absence of 18α-glycyrrhetinic acid (18aGA). **d** Acetylcholine (Ach)-induced dilatation in K^+-preconstricted mesenteric arteries with and without L-NAME from WT and Cav3.1$^{-/-}$ mice. Data are means±SEM, n=6;*P<0.05

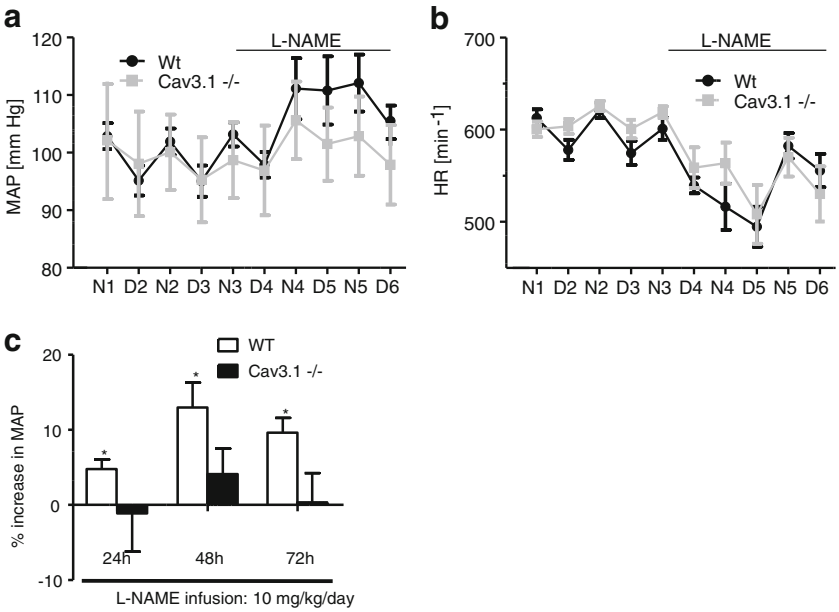

Fig. 3 Effect of L-NAME on mean arterial blood pressure (MAP) in Cav3.1$^{-/-}$ mice. **a** MAP measured by indwelling catheters over 6 days and nights with L-NAME infusion in WT and Cav3.1$^{-/-}$ mice. **b** Heart rate (*HR*) measured over 6 days and nights with L-NAME infusion in WT and Cav3.1$^{-/-}$ mice. **c** Average increase in MAP from basal values (average of all measured values for the time period without L-NAME infusion) to 24, 48 and 72 h after start of L-NAME infusion in WT and Cav3.1$^{-/-}$ mice. Data are means±SEM, n= 6. *Asterisk* indicates significant increase in MAP compared to baseline (P<0.05)

judged by CD31 mRNA abundance was not different between arteries of the two genotypes (Online Resource 3c).

The Cav1.2 mRNA level was not different in mesenteric arteries from Cav3.1$^{-/-}$ compared to wild type mice (Online Resource 3d). Furthermore, the expression level of Cav3.2 was not changed in Cav3.1$^{-/-}$ compared to wild type mice (Online Resource 3e).

Discussion

NO is one of the most important factors for relaxation of blood vessels and changes in NO bioavailability will affect blood flow and arterial blood pressure. The present study shows that NO-mediated dilatation during depolarization of resistance vessels involves activation of Cav3.1 T-type channels. Cav3.1

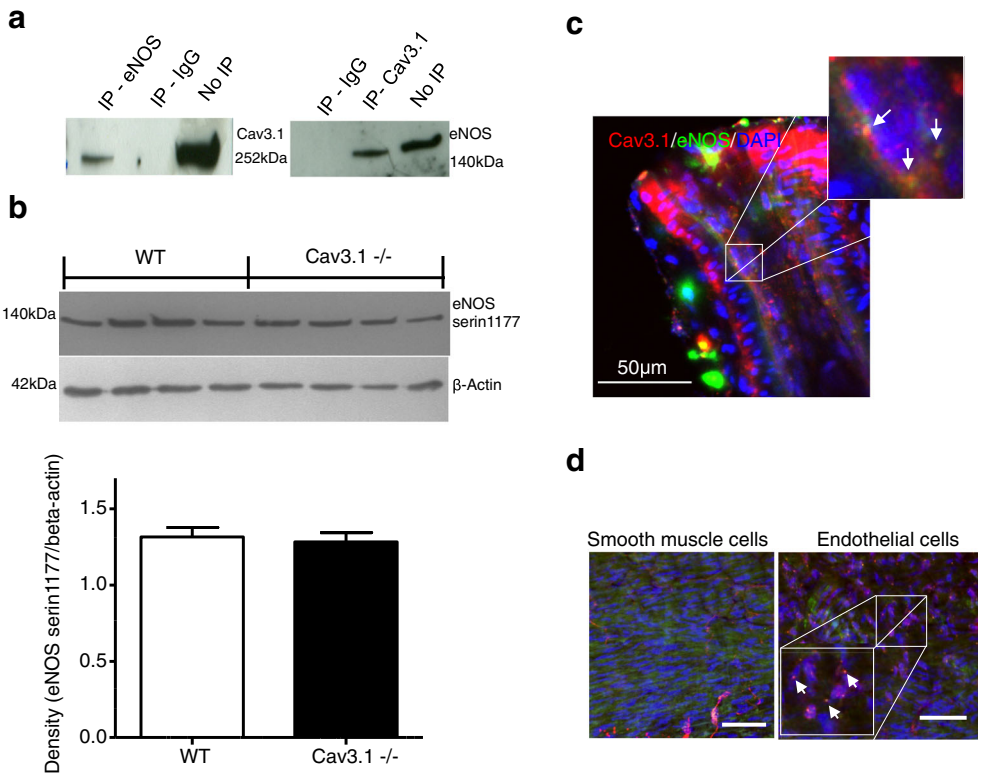

Fig. 4 Co-localization of Cav3.1 and eNOS. **a** Immunoprecipitation of eNOS from mouse aorta homogenates showed that Cav3.1 coprecipitated with eNOS (*left panel*), and immunoprecipitation of Cav3.1 showed that eNOS coprecipitated with Cav3.1. **b** Serine 1177 phosphorylated eNOS protein levels in isolated aorta from WT and Cav3.1$^{-/-}$ mice measured by Western blotting. **c** Immunostaining of isolated mesenteric arteries for Cav3.1 (*red*) and eNOS (*green*). Cav3.1 appears to co-localize with eNOS in the endothelial cells (*arrows*). **d** Immunostaining of isolated aortas for Cav3.1 (*green*) and eNOS (*red*). The *inset* shows that Cav3.1 appears to co-localize with eNOS in the endothelial cells (*arrows*). *Bar* 50 µm

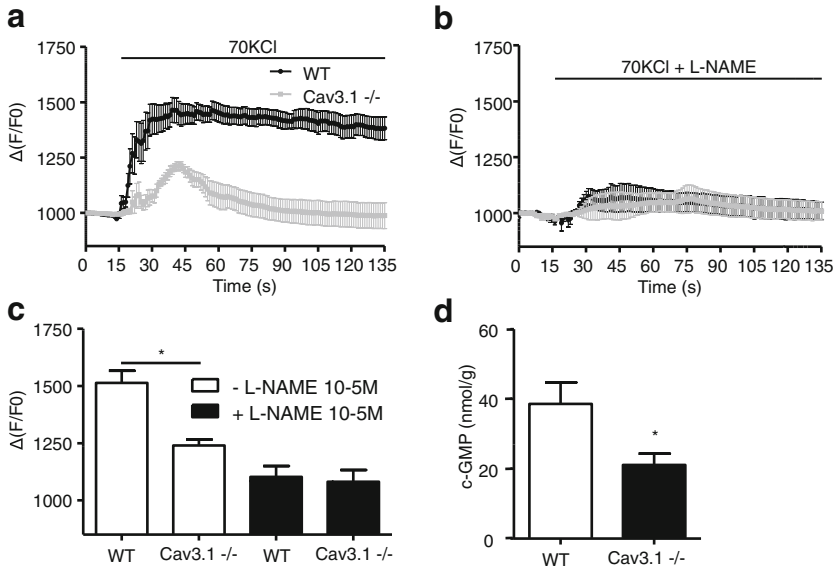

Fig. 5 NO and cyclic GMP levels from Cav3.1-deficient mice are affected by depolarization. **a** Average time tracings of DAF-FM fluorescent imaging measurements from mesenteric vessels from WT and Cav3.1$^{-/-}$ mice, n=9 and 6 with 2–3 endothelial cells measured per experiment. **b** Average time tracings of DAF-FM fluorescence in the presence of the eNOS inhibitor L-NAME, n=4 and three for WT and Cav3.1$^{-/-}$, respectively. **c** Max NO levels are significantly attenuated in Cav3.1$^{-/-}$ compared to WT in response to 70 mM K^+, and the increase is abolished by L-NAME. **d** A significantly lower level of cyclic GMP was detected in aortae from Cav3.1$^{-/-}$ mice compared to WT after depolarization (HPS 70 mM). Data are means±SEM, n=5; *P<0.05

and eNOS were co-localized and diminished calcium influx in Cav3.1$^{-/-}$ mice might lead to the observed attenuated NO and cGMP formation after depolarization. Furthermore, the contribution of NO to the regulation of blood pressure also involves T-type channels.

The secondary dilatation investigated here is NO-dependent as it was inhibited by L-NAME and was absent in eNOS$^{-/-}$ mice. In agreement, it has previously been shown that Cav3 channels are involved in NO-dependent vasodilatations of the renal efferent arteriole since they were inhibited by T-type channel blockers [17]. Furthermore, exogenous NO administration by the NO donor SNP dilated the Cav3.1$^{-/-}$ vessels significantly suggesting that the vascular smooth muscle cells had a normal relaxation mechanism but a changed endothelial cell function. In wild type mice, SNP dilated the vessels by only 10 % which was probably due to the fact that vessels were already spontaneously dilated. Cav3.2 channels are also found in the endothelium of mesenteric blood vessels [5] and may play a role in vasodilatation [6, 12, 7]. The impaired relaxation of coronary vessels of Cav3.2$^{-/-}$ mice in response to acetylcholine and sodium nitroprusside probably results from coupling of Cav3.2 channels to BK_{ca} channels in the vascular smooth muscle cells [6]. Such coupling is unlikely to explain the present findings for Cav3.1 channels, as BK_{ca} channels would not be activated during the clamped depolarization exerted by HPS. The same holds true for relaxations due to endothelium-dependent hyperpolarization. Therefore, the vasodilatation investigated in the present study must depend on a depolarization-induced activation of eNOS that requires opening of T-Type channels.

The co-localization of Cav3.1 with eNOS in the endothelium may explain the decreased dilator response and lower blood pressure response in Cav3.1$^{-/-}$ mice after infusion of L-NAME. The complex between Cav3.1 and eNOS could provide a route by which activation of T-type channels in response to depolarization leads to calcium influx resulting in an increased intracellular calcium concentration in the immediate vicinity of eNOS, subsequent activation of the enzyme and NO production. In accordance with the present findings, earlier observations suggested not only the presence of functional voltage-gated calcium channels but actually the expression of Cav3 in the endothelium [5, 33, 16]. The present study demonstrates both the presence of, and a function for Cav3.1 in endothelial cells of systemic arteries of the mouse. Likewise, Cav3.1 is present in pulmonary endothelial cells and changes in intracellular endothelial calcium in response to hypoxia are lacking in Cav3.1$^{-/-}$ mice [32]. Cav3.1 and eNOS do not only co-localize in the endothelium of mouse mesenteric arteries (present study) but also in cardiac myocytes, where Cav3.1 and subsequent NOS activation are involved in the protection of the heart against hypertrophy [20]. However, regulation of eNOS through phosphorylation is not affected by T-type calcium channels implying that it is the direct increase in the calcium concentration that activates the enzyme [20]. We suggest, that also in the endothelium, Cav3.1 directly activates eNOS by a local change in calcium concentration.

The eNOS-dependent nature of the endothelium-dependent effect of Cav3.1 channels was confirmed by determining the production of both NO and cGMP. Measurements of NO levels by DAF-FM showed that the amount of NO produced

after depolarization was smaller in blood vessels of the Cav3.1 knock-out compared to those of wild type animals. In agreement, the cGMP levels were also lower in the former. It therefore seems reasonable to conclude that depolarization lead to opening of Cav3.1 T-type channels resulting in activation of the NO-cGMP pathway.

The activation of eNOS could potentially also involve signaling from vascular smooth muscle to endothelial cells via the passage of calcium through myoendothelial gap junctions after depolarization of the smooth muscle cells. Indeed, an increased calcium concentration in vascular smooth muscle can elevate the concentration of the activator ion in endothelial cells [15]. In rabbit afferent arterioles, depolarization increases the intracellular calcium concentration in the smooth muscle cells, which is then followed by calcium increase in the endothelium where it stimulates NO production [30]. However, in the present study, a gap junction inhibitor did not significantly affect the secondary vasodilatation following depolarization, making intercellular transport of Ca^{2+} unlikely. The tested response using high potassium as constrictor probably is nonphysiological. However, it allows investigating a phenomenon that is of physiological relevance in vivo as can be concluded from the present arterial blood pressure data. Therefore, the T-type dependent dilatation is a phenomenon that occurs probably only during depolarization of endothelial cells as dilatations resulting from either endothelium-dependent (acetylcholine) or endothelium-independent (isoprenaline) hyperpolarizations were not affected by the absence of T-type channels.

The depolarization-induced constriction was not significantly different between genotypes which were probably not due to compensation via upregulation of other calcium channels as there was no change in Cav1.2 or Cav3.2 mRNA levels between knock-out and wild type animals. In agreement, L-type and T-type (Cav3.2) currents are not changed due to lack of Cav3.1 currents in the $Cav3.1^{-/-}$ mouse [19]. Chronic NO deficiency augments the T-type channel contribution to vascular tone and both Cav3.1 and Cav3.2 are involved in the phenylephrine-induced constriction [14]. However, in the present study, these contractile effects were not seen following depolarization with high potassium solution since constrictions did not differ amongst the genotypes. This is likely due to inactivation of these T-type channels at the depolarized potentials produced by the high potassium solution [4]. The continued activity of the T-type channels responsible for the vasodilatation described here may suggest the involvement of T-type channel splice variants with a more "depolarized" profile [17, 16].

The present in vivo data show that lack of Cav3.1 T-type channels has no impact on baseline arterial blood pressure or its diurnal variations. However, the heart rate is lower in $Cav3.1^{-/-}$ due to a changed decreased atrioventricular conduction in the heart [19] although this was not observed in the present L-NAME experiment. The reason for the lack of a significant lower heart rate in the present study is not clear, but the used strain does exhibit a lower heart rate when measured over 2 weeks. On the other hand, $Cav3.1^{-/-}$ mice were resistant to L-NAME treatment. The absence of a blood pressure increase in the $Cav3.1^{-/-}$ mouse after L-NAME treatment is in agreement with a direct connection between Cav3.1 and the activation of eNOS in the vascular wall. Thus, activation of T-type calcium channels in the endothelium may serve as a protective role to promote NO-dependent dilatation after strong depolarizing contractile stimuli in resistance vessels.

T-type channel blockers have superior renoprotective effects compared with L-type calcium blockers and T-type channels are an important therapeutic target, with selective blockers possibly providing an additional tool for treating hypertensive proteinuric kidney disease [8]. However, only a few human studies with T-type channel calcium antagonists have been reported, and they provide no information on endothelial function. Treatment with combined L- and T-type antagonists yields greater efficacy than amlodipine (L-type antagonist) in reducing arterial blood pressure and proteinuria [22, 25, 23]. The T-type antagonist efonidipine slows the progression of proteinuric kidney disease in a way similar to that of angiotensin-converting enzyme inhibitors [13]. However, the demonstration in the present study that Cav3.1 T-type deletion can reduce NO-dependent vasodilatations and that this may be a generalized vascular phenomenon. These data therefore need to be taken into account when T-type blockers are considered for the treatment of obesity [29], hypertension [22] and cancer [27].

Acknowledgments We would like to thank Lis Teusch and Vivi Monrad for expert technical assistance. Also, we thank Philippe Lory, University de Montpellier, INSERM U661, France for back crossing the $Cav3.1^{-/-}$ mice into a C57BL/6 background. This work was supported by grants from the Danish Medical Research Council (11-107552), The Danish Heart Foundation (11-04-R84-A3492-22663) and Aase and Ejnar Danielsens Foundation. The bioimaging experiments reported in this paper were performed at DaMBIC, a bioimaging research core facility, at the University of Southern Denmark. DaMBIC was established by an equipment grant from the Danish Agency for Science Technology and Innovation and by internal funding from the University of Southern Denmark

Conflict of interest None.

References

1. Abd El-Rahman RR, Harraz OF, Brett SE, Anfinogenova Y, Mufti RE, Goldman D, Welsh DG (2012) Identification of L- and T-type Ca^{2+} channels in rat cerebral arteries: role in myogenic tone development. Am J Physiol Heart Circ Physiol 304(1):H58–H71. doi:10.1152/ajpheart.00476.2012
2. Andersen H, Jaff MG, Hogh D, Vanhoutte P, Hansen PB (2011) Adenosine elicits an eNOS-independent reduction in arterial blood

pressure in conscious mice that involves adenosine A2A receptors. Acta Physiol (Oxf) 203(1):197–207
3. Ball CJ, Wilson DP, Turner SP, Saint DA, Beltrame JF (2009) Heterogeneity of L- and T-channels in the vasculature: rationale for the efficacy of combined L- and T-blockade. Hypertension 53(4): 654–660
4. Bjorling K, Morita H, Olsen MF, Prodan A, Hansen PB, Lory P, Holstein-Rathlou NH, Jensen LJ (2013) Myogenic tone is impaired at low arterial pressure in mice deficient in the low-voltage-activated Ca(V) 3.1 T-type Ca(2+) channel. Acta Physiol (Oxf)
5. Braunstein TH, Inoue R, Cribbs L, Oike M, Ito Y, Holstein-Rathlou NH, Jensen LJ (2008) The role of L- and T-type calcium channels in local and remote calcium responses in rat mesenteric terminal arterioles. J Vasc Res 46(2):138–151
6. Chen CC, Lamping KG, Nuno DW, Barresi R, Prouty SJ, Lavoie JL, Cribbs LL, England SK, Sigmund CD, Weiss RM, Williamson RA, Hill JA, Campbell KP (2003) Abnormal coronary function in mice deficient in alpha1H T-type Ca2+ channels. Science 302(5649): 1416–1418
7. Figueroa XF, Chen CC, Campbell KP, Damon DN, Day KH, Ramos S, Duling BR (2007) Are voltage-dependent ion channels involved in the endothelial cell control of vasomotor tone? Am J Physiol Heart Circ Physiol 293(3):H1371–H1383. doi:10.1152/ajpheart.01368.2006
8. Hansen PB (2013) Functional and pharmacological consequences of the distribution of voltage-gated calcium channels in the renal blood vessels. Acta Physiol (Oxf) 207(4):690–699
9. Hansen PB, Hristovska A, Wolff H, Vanhoutte P, Jensen BL, Bie P (2010) Uridine adenosine tetraphosphate affects contractility of mouse aorta and decreases blood pressure in conscious rats and mice. Acta Physiol (Oxf) 200(2):171–179
10. Hansen PB, Jensen BL, Andreasen D, Skott O (2001) Differential expression of T- and L-type voltage-dependent calcium channels in renal resistance vessels. Circ Res 89(7):630–638
11. Hansen PB, Poulsen CB, Walter S, Marcussen N, Cribbs LL, Skott O, Jensen BL (2011) Functional importance of L- and p/q-type voltage-gated calcium channels in human renal vasculature. Hypertension 58 (3):464–470
12. Harraz OF, Brett SE, Welsh DG (2014) Nitric oxide suppresses vascular voltage-gated T-type Ca2+ channels through cGMP/PKG signaling. Am J Physiol Heart Circ Physiol 306(2):H279–H285. doi:10.1152/ajpheart.00743.2013
13. Hayashi K, Kumagai H, Saruta T (2003) Effect of efonidipine and ACE inhibitors on proteinuria in human hypertension with renal impairment. Am J Hypertens 16(2):116–122
14. Howitt L, Kuo IY, Ellis A, Chaston DJ, Shin HS, Hansen PB, Hill CE (2013) Chronic deficit in nitric oxide elicits oxidative stress and augments T-type calcium channel contribution to vascular tone of rodent arteries and arterioles. Cardiovasc Res
15. Isakson BE, Ramos SI, Duling BR (2007) Ca2+ and inositol 1,4,5-trisphosphate-mediated signaling across the myoendothelial junction. Circ Res 100(2):246–254
16. Kuo IY, Ellis A, Seymour VA, Sandow SL, Hill CE (2010) Dihydropyridine-insensitive calcium currents contribute to function of small cerebral arteries. J Cereb Blood Flow Metab 30(6):1226–1239. doi:10.1038/jcbfm.2010.11
17. Kuo IY, Wolfle SE, Hill CE (2011) T-type calcium channels and vascular function: the new kid on the block? J Physiol 589(Pt 4):783–795
18. Lee J, Kim D, Shin HS (2004) Lack of delta waves and sleep disturbances during non-rapid eye movement sleep in mice lacking alpha1G-subunit of T-type calcium channels. Proc Natl Acad Sci U S A 101(52):18195–18199. doi:10.1073/pnas.0408089101
19. Mangoni ME, Traboulsie A, Leoni AL, Couette B, Marger L, Le Quang K, Kupfer E, Cohen-Solal A, Vilar J, Shin HS, Escande D, Charpentier F, Nargeot J, Lory P (2006) Bradycardia and slowing of the atrioventricular conduction in mice lacking CaV3.1/alpha1G T-type calcium channels. Circ Res 98(11):1422–1430
20. Nakayama H, Bodi I, Correll RN, Chen X, Lorenz J, Houser SR, Robbins J, Schwartz A, Molkentin JD (2009) alpha1G-dependent T-type Ca2+ current antagonizes cardiac hypertrophy through a NOS3-dependent mechanism in mice. J Clin Invest 119(12):3787–3796
21. Navarro-Gonzalez MF, Grayson TH, Meaney KR, Cribbs LL, Hill CE (2009) Non-L-type voltage-dependent calcium channels control vascular tone of the rat basilar artery. Clin Exp Pharmacol Physiol 36(1):55–66
22. Ohishi M, Takagi T, Ito N, Terai M, Tatara Y, Hayashi N, Shiota A, Katsuya T, Rakugi H, Ogihara T (2007) Renal-protective effect of T- and L-type calcium channel blockers in hypertensive patients: an Amlodipine-to-Benidipine Changeover (ABC) study. Hypertens Res 30(9):797–806
23. Ohta M, Sugawara S, Sato N, Kuriyama C, Hoshino C, Kikuchi A (2009) Effects of benidipine, a long-acting T-type calcium channel blocker, on home blood pressure and renal function in patients with essential hypertension: a retrospective, 'real-world' comparison with amlodipine. Clin Drug Investig 29(11):739–746
24. Poulsen CB, Al-Mashhadi RH, Cribbs LL, Skott O, Hansen PB (2011) T-type voltage-gated calcium channels regulate the tone of mouse efferent arterioles. Kidney Int 79(4):443–451. doi:10.1038/ki.2010.429
25. Sasaki H, Saiki A, Endo K, Ban N, Yamaguchi T, Kawana H, Nagayama D, Ohhira M, Oyama T, Miyashita Y, Shirai K (2009) Protective effects of efonidipine, a T- and L-type calcium channel blocker, on renal function and arterial stiffness in type 2 diabetic patients with hypertension and nephropathy. J Atheroscler Thromb 16(5):568–575
26. Shcheglovitov A, Vitko I, Bidaud I, Baumgart JP, Navarro-Gonzalez MF, Grayson TH, Lory P, Hill CE, Perez-Reyes E (2008) Alternative splicing within the I–II loop controls surface expression of T-type $Ca_v3.1$ calcium channels. FEBS Lett 582(27):3765–3770. doi:10.1016/j.febslet.2008.10.013
27. Taylor JT, Huang L, Pottle JE, Liu K, Yang Y, Zeng X, Keyser BM, Agrawal KC, Hansen JB, Li M (2008) Selective blockade of T-type Ca2+ channels suppresses human breast cancer cell proliferation. Cancer Lett 267(1):116–124. doi:10.1016/j.canlet.2008.03.032
28. Tzeng BH, Chen YH, Huang CH, Lin SS, Lee KR, Chen CC (2012) The Ca(v)3.1 T-type calcium channel is required for neointimal formation in response to vascular injury in mice. Cardiovasc Res 96(3):533–542. doi:10.1093/cvr/cvs257
29. Uebele VN, Gotter AL, Nuss CE, Kraus RL, Doran SM, Garson SL, Reiss DR, Li Y, Barrow JC, Reger TS, Yang ZQ, Ballard JE, Tang C, Metzger JM, Wang SP, Koblan KS, Renger JJ (2009) Antagonism of T-type calcium channels inhibits high-fat diet-induced weight gain in mice. J Clin Invest 119(6):1659–1667. doi:10.1172/JCI36954
30. Uhrenholt TR, Schjerning J, Vanhoutte PM, Jensen BL, Skott O (2007) Intercellular calcium signaling and nitric oxide feedback during constriction of rabbit renal afferent arterioles. Am J Physiol Renal Physiol 292(4):F1124–F1131. doi:10.1152/ajprenal.00420.2006
31. Vitko I, Bidaud I, Arias JM, Mezghrani A, Lory P, Perez-Reyes E (2007) The I–II loop controls plasma membrane expression and gating of $Ca_v3.2$ T-type Ca^{2+} channels: a paradigm for childhood absence epilepsy mutations. J Neurosci 27(2):322–330
32. Wang L, Yin J, Nickles HT, Ranke H, Tabuchi A, Hoffmann J, Tabeling C, Barbosa-Sicard E, Chanson M, Kwak BR, Shin HS, Wu S, Isakson BE, Witzenrath M, de Wit C, Fleming I, Kuppe H, Kuebler WM (2012) Hypoxic pulmonary vasoconstriction requires connexin 40-mediated endothelial signal conduction. J Clin Invest 122(11):4218–4230. doi:10.1172/JCI59176
33. Wu S, Haynes J Jr, Taylor JT, Obiako BO, Stubbs JR, Li M, Stevens T (2003) Cav3.1 (α1G) T-type Ca^{2+} channels mediate vaso-occlusion of sickled erythrocytes in lung microcirculation. Circ Res 93(4):346–353